Is the spin transition in Fe2+-bearing perovskite visible in seismology?

Razvan Caracas, David Mainprice, Christine Thomas

GEOPHYSICAL RESEARCH LETTERS, VOL. 37, L13309, doi:10.1029/2010GL043320, 2010

Is the spin transition in Fe^{2+}-bearing perovskite visible in seismology?

Razvan Caracas,[1] David Mainprice,[2] and Christine Thomas[3]

Received 18 March 2010; revised 5 June 2010; accepted 14 June 2010; published 15 July 2010.

[1] We determine the elasticity of $FeSiO_3$ perovskite for various spin configurations using density-functional theory calculations. The elastic moduli and the bulk seismic wave velocities are weakly affected by the spin transition. However we show that the intrinsic differences in seismic anisotropy between the high-spin and low-spin phases of Fe-bearing perovskite coupled with lattice preferred orientation that can develop due and during the convection may lead to distinct seismic signatures between the top and the bottom of the lower mantle. These signatures should be detectable in observations and they need to be taken into account in tomographic studies of the Earth's lower mantle. **Citation:** Caracas, R., D. Mainprice, and C. Thomas (2010), Is the spin transition in Fe^{2+}-bearing perovskite visible in seismology?, *Geophys. Res. Lett.*, *37*, L13309, doi:10.1029/2010GL043320.

1. Introduction

[2] It is now well established that the Fe-bearing minerals exhibit spin transitions under pressure. Magnesiowustite has been extensively studied form both experimental and computational points of view and its phase diagram and spin transition have been thoroughly mapped out [e.g., *Lin et al.*, 2005; *Lin and Tsuchiya*, 2008]. In the last years more and more evidence emerged, from both experimental and theoretical sides, that points to a magnetic phase transition also in Fe^{2+}-bearing perovskite [*Badro et al.*, 2004; *McCammon et al.*, 2008; *Lin et al.*, 2007] and post-perovskite [*Lin et al.*, 2008] at high-pressure. The change in Mössbauer signal [*McCammon et al.*, 2008; *Lin et al.*, 2008] and X-ray emission spectra [*Badro et al.*, 2004; *Lin et al.*, 2008] over a narrow pressure range have been interpreted as the signature of the spin transition, though there is current disagreement between the different experimental groups regarding this interpretation. Other experimental studies observed a continuous spin transition from high-spin state to low-spin state for ferrous iron for both perovskite [*Li et al.*, 2004, 2006] and post-perovskite [*Jackson et al.*, 2009], but ferric iron might remain in a high-spin state, while another set of experiments observe the persistence of non-vanishing spin up to high pressure in perovskite [*Jackson et al.*, 2005].

[3] First-principles calculations based on density functional theory (DFT) suggest that Fe-bearing $MgSiO_3$ perovskite undergoes a spin transition from high-spin state to low-spin state [*Bengtson et al.*, 2008; *Stackhouse et al.*, 2007; *Umemoto et al.*, 2008]. The transition pressure is highly dependent on the iron content: up to about 25% Fe the transition pressure remains constant while at iron concentrations larger than about 25% the transition pressure decreases dramatically with increasing iron content [*Bengtson et al.*, 2008]. The spin transition is associated with a structural distortion: the volume collapse of the iron atoms due to the electron pairing is accommodated in the structure by a displacement that breaks the symmetry of the structure and changes the local coordination environment [*Bengtson et al.*, 2008; *Umemoto et al.*, 2008]. Non-randomized structures obtained only from replacement of Mg by Fe in the Pbnm structure lead to much higher transition pressures [*Stackhouse et al.*, 2007; *Caracas and Cohen*, 2005; *Fang and Ahuja*, 2008] or to iron disproportionation [*Zhang and Oganov*, 2006].

[4] Using a different approach than in the previous theoretical studies, recently we investigated the dynamical stability of Pbnm $FeSiO_3$ perovskite and show the existence of unstable phonon modes. Following their corresponding eigendisplacements we found various monoclinic and triclinic configurations with intermediate spin state competitive to the high-spin antiferromagnetic structure and eventually a triclinic low-spin structure, which is the stable phase above about 37 GPa. The intermediate spin structures exhibit only minor displacements relative to the high-spin orthorhombic structures, while the triclinic low-spin structure is strongly distorted. Consequently we focus in the following only on the high-spin ferro-, antiferro-magnetic and the low-spin structures as most representative for the $FeSiO_3$ perovskite system at pressures characteristic to the lower mantle.

2. Computational Details

[5] Hereinafter we understand by high-spin, intermediate-spin and low-spin states the electronic configurations with a net residual magnetic moment of respectively, 4, 2 and 0 Bohr magnetons for each Fe atom, equivalent to 4, 2 and 0 unpaired d electrons per Fe site. This is quite an artificial and simplified way of representing magnetization, especially in metallic systems where orbital hybridization and electron delocalization due both to the lattice periodicity and the metallic character of the bonding oftentimes lead to non-integer Fermi band occupations and thus to non-integer values of the remnant magnetization.

[6] We use density-functional theory [*Hohenberg and Kohn*, 1964; *Kohn and Sham*, 1965] in the ABINIT implementation [*Gonze et al.*, 2002, 2005b, 2009], which is based on planewaves and pseudopotentials. We perform all the

[1] Laboratoire de Sciences de la Terre, UMR 5570, Ecole Normale Supérieure de Lyon, CNRS, Lyon, France.
[2] Géosciences Montpellier, UMR 5243, Université Montpellier 2, CNRS, Montpellier, France.
[3] Institut für Geophysik, Westfälische Wilhelms Universität Münster, Münster, Germany.

0094-8276/10/2010GL043320

Table 1. Single-Crystal Elastic Constants and Bulk Elastic Moduli and Bulk Seismic Wave Velocities for Homogeneous Aggregates for $FeSiO_3$ Perovskite in Low-Spin and Two High-Spin Magnetic Configurations[a]

	$FeSiO_3$ - LS	$FeSiO_3$ - FM	$FeSiO_3$ - AFM
C11	973	880	914
C22	1041	953	953
C33	1081	936	940
C12	561	494	484
C13	444	443	427
C23	421	471	472
C44	228	296	295
C55	245	233	230
C66	283	214	209
RHO (g/cm^3)	6.827	6.560	6.565
K (Gpa)	660	620	619
G (GPa)	259	237	240
Y(GPa)	688	631	638
μ	0.31	0.33	0.33
Vp (km/s)	12.14	11.95	11.96
Vs (km/s)	6.16	6.01	6.05

[a]Results obtained from static calculations at 90 GPa. For the triclinic structure we only list the non-zero constants.

static calculations using the planar-augmented wavefunction (PAW) formalism. Then for the relaxed structures we compute the full elastic constants tensor and the phonons in the Brillouin zone center in the framework of the density functional perturbation theory (DFPT) [*Baroni et al.*, 1987; *Gonze and Lee*, 1997; *Baroni et al.*, 2001; *Gonze et al.*, 2005a] using standard norm-conserving Troullier-Martins pseudopotentials. Here the elastic constants are expressed as the derivative of the energy with respect to lattice strains [*Hamann et al.*, 2005]. The atomic relaxations due to strain are taken into account from the phonon and dielectric calculations by inverting a matrix containing the interatomic force constants, the couplings with the strains and the couplings with the electric fields.

[7] We use the local density approximation for the exchange-correlation energy both DFT and DFPT calculations. As usual with planewave basis sets, the numerical accuracy of the calculation can be improved by increasing the cut-off kinetic energy of the planewaves and the density of the sampling of the Brillouin zone [*Payne et al.*, 1992]. Here we use a 35 Eh cut-off energy for the kinetic energy of the planewaves. We sample the reciprocal space using a $6 \times 6 \times 6$ regular grid of special k points according to the Monkhorst-Pack scheme [*Monkhorst and Pack*, 1976]. These parameters ensure a precision of the calculation better than 1 mEh per unit cell in energy and better than 1GPa in pressure.

3. Results and Discussion

[8] Because Fe-bearing perovskite is the major mineral of the Earth's lower mantle it obviously received a particular attention form both the experimental and computational community. The elastic constants of $MgSiO_3$ perovskite have been previously reported in several theoretical [e.g., *Cohen*, 1987; *Karki et al.*, 1998; *Oganov et al.*, 2001; *Wentzcovitch et al.*, 2004; *Caracas and Cohen*, 2005, 2007] and experimental [*Yeganeh-Haeri et al.*, 1989; *Sinelnikov et al.*, 1998] studies. The seismic properties of a homogeneous aggregate of perovskite are close to the values estimated for PREM though not identical, and corrections due to at least to temperature, chemical composition, redox state of iron and iron spin state need to be considered to account for these discrepancies. However many of these corrections are still unknown. In this paper we discuss in detail the effect on the seismic properties of the iron spin transition in perovskite.

[9] The elasticity of the $(Mg,Fe)SiO_3$ perovskite has been addressed so far considering only the high-spin state of iron. Two approaches were used. First is to compute the elastic tensors of the end member $MgSiO_3$ and $FeSiO_3$ terms and perform a linear interpolation along the solid solution. These studies [*Li et al.*, 2005; *Caracas and Cohen*, 2005, 2007, 2008; *Stackhouse et al.*, 2006] showed that the effect of iron is to lower both the compressional and the shear seismic wave velocities. For average pyrolitic compositions (10% ferrous iron on the Mg site) the decrease in velocities is of about 0.17 km/s at 120 GPa [*Caracas and Cohen*, 2005, 2007], which corresponds to reduction with respect to pure $MgSO_3$. The second approach is to effectively build the crystal structures with the desired Fe content by replacing Mg with ferrous iron [*Kiefer et al.*, 2002]. This latter approach is more correct, but is more computationally intensive while the departure from linear scaling along the solid solution might be very small. Here we use the first approach, computing the elastic constants tensor for the $FeSiO_3$ term and studying the differences between various spin states.

[10] $MgSiO_3$ perovskite has an orthorhombic structure with 20 atoms per unit cell and Pbnm space group. The structure exhibits a three-dimensional network of SiO_6 octahedra, each two neighboring octahedra sharing one oxygen atom along each of the cartesian directions, and the larger Mg cations sitting in the interoctahedral space. It has 9 independent elastic constants: C_{11}, C_{22}, C_{33}, C_{12}, C_{13}, C_{23}, C_{44}, C_{55} and C_{66}.

[11] For the $FeSiO_3$ end-member term we consider both the ferromagnetic (FM) and the antiferromagnetic (AFM) configurations, even though the latter one is the most stable; the energy difference between the two is of about 5 mHa per formula unit and is weakly dependent of the pressure [*Caracas and Cohen*, 2005]. This corresponds to roughly 1000K, meaning that at mantle conditions the two configurations can coexist. When performing the calculations we impose a residual magnetic moment of 4 magneton-Bohrs for each Fe site in case of the FM configuration. The magnetic moment for the AFM is allowed to freely relax and settles to 3.4 magneton-Bohrs at 90 GPa; it is weakly varying with pressure. For the low-spin structure the calculation is non-spin-polarized. The FM and AFM magnetic structures are metallic and have orthorhombic symmetry and the LS is insulating with triclinic symmetry.

[12] Table 1 lists the elastic constants, the density and the bulk seismic properties computed for the FM, AFM and the LS structures of $FeSiO_3$ at 90 GPa. Except for C_{12}, C_{13} and C_{23}, all the off-diagonal elastic constants of the triclinic LS structure are smaller than 1 GPa. Essentially the triclinic distortions allow only a rearrangement of the structure to accommodate the smaller low-spin Fe ions, but preserves the quasi-orthorhombic character of the lattice.

[13] The differences between the FM and AFM elastic constants tensors are minimal. The largest discrepancies

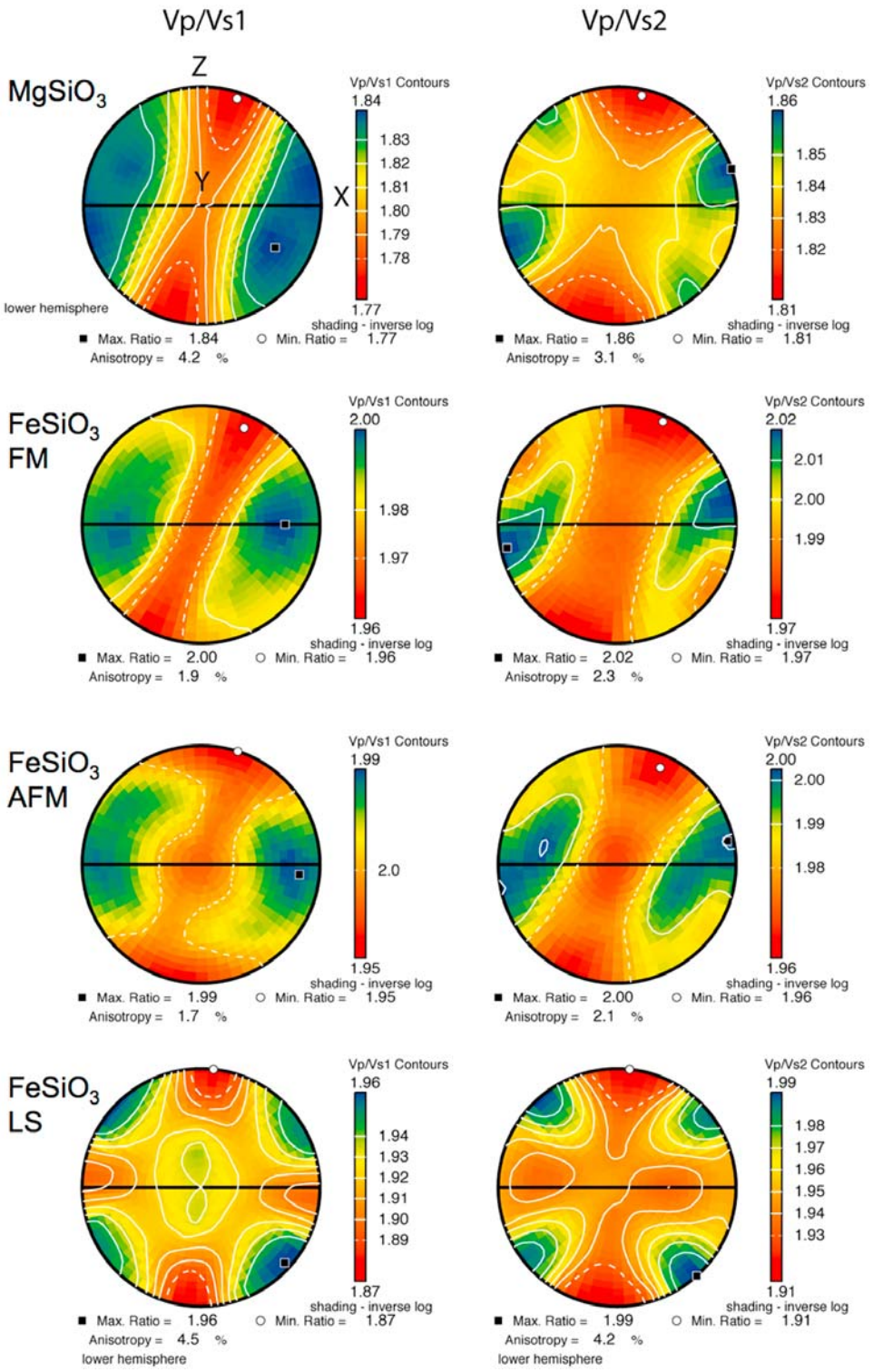

Figure 1. The predicted seismic anisotropy for Vp and Vs for $MgSiO_3$ and $FeSiO_3$ perovskites with various spin configurations for polycrystalline aggregates, based on single crystal elastic constants reported in Table 1 and VPSC predicted crystal preferred orientations for $MgSiO_3$ in simple shear for a shear strain of 1.73. The Voigt-Ruess-Hill average was used for elastic properties. X, Y and Z are the finite strain axes.

are on the C_{11} and C_{13} constants, of respectively −34 and +16 GPa, while all the others are less than 10 GPa. The difference of density is on the order of 0.01 g/cm^3, of the elastic moduli less than 3, resulting in quasi-identical bulk seismic velocities for homogeneous aggregates. On the other hand the differences between the high-spin and the low-spin structures are considerable, going as high as 141 GPa for the C_{33} elastic constant. The density difference is also significant with the LS structure denser by 0.26 g/cm$_3$ than the AFM, namely almost 4%. The change in density is correctly

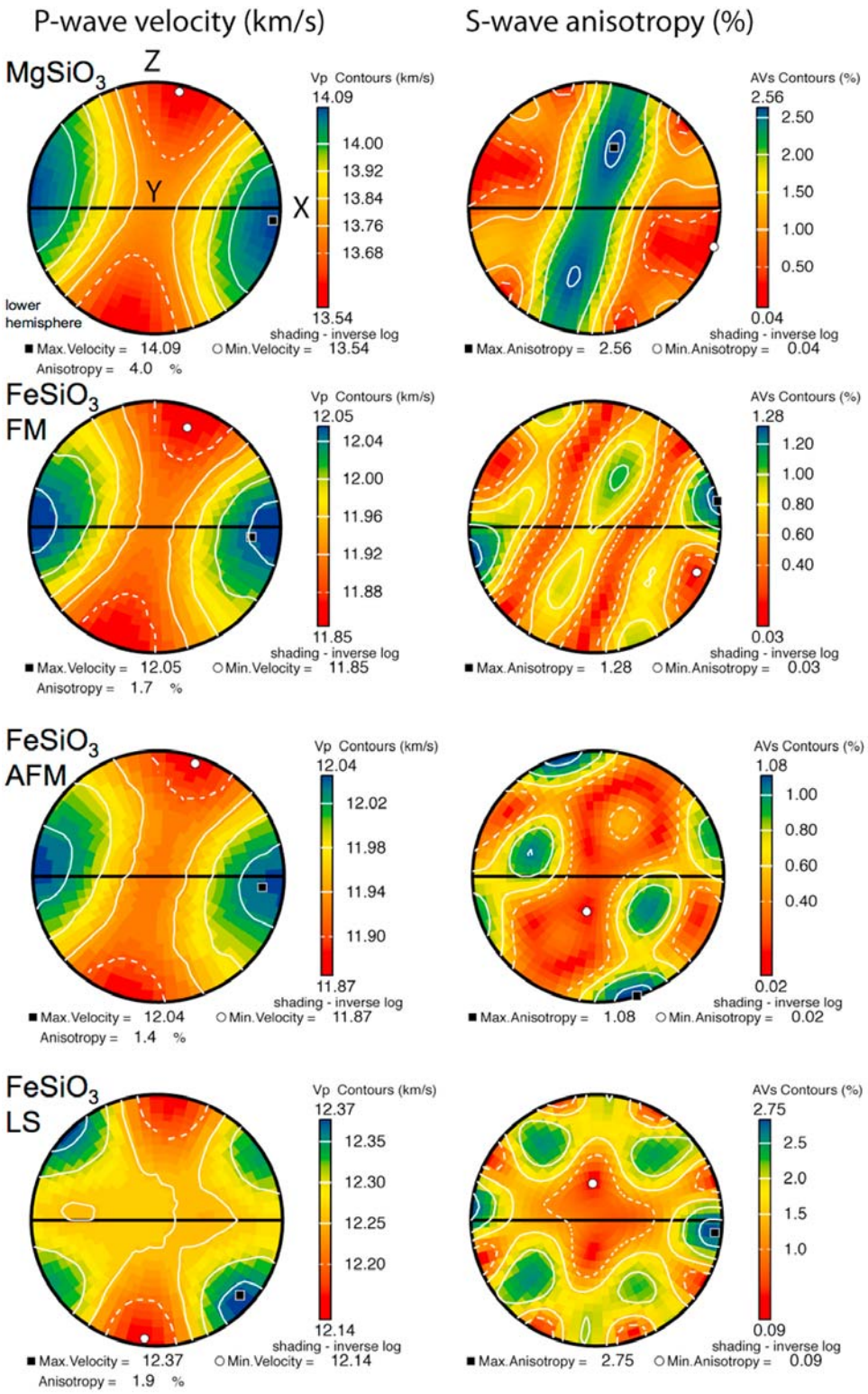

Figure 2. The predicted seismic anisotropy for various spin configurations in pure $FeSiO_3$ and $MgSiO_3$ perovskite coupled with lattice preferred orientation. We use the computed elastic constants from Table 1 for $FeSiO_3$ at 90 GPa and 0 K and the experimental measurements at room temperature and 90 GPa for $MgSiO_3$. The LS configuration has distinctively low values (red) along the normal (Z direction) to the flow (XY) plane and in the flow plane (XY).

represented in changes in elastic moduli and seismic wave velocities, with larger values for LS structure. The absolute differences are larger for the bulk moduli (K), on the order of about 41–42 GPa, than for the shear moduli (G), on the order of 19–22 GPa. The Young modulus, defined as $Y = (9KG)/(3K+G)$ shows similar values between FM and AFM that are lower than LS by about 50 GPa. The Poisson ratio, $\mu = Y/2G - 1$, is in the range 0.31–0.33 for all the structures at

90 GPa, larger than most ceramics, but usual for Fe-bearing perovskites at high pressure [*Caracas and Cohen*, 2007].

[14] In terms of seismic wave velocities for homogeneous bulk aggregates the FM and AFM are hardly distinguishable with differences on the order of 0.01 km/s for compressional wave velocities (Vp) and 0.04 km/s for shear wave velocities (Vs). The differences are more important with respect to the LS structure, through which the Vp travel with 0.18 km/s faster than in AFM and the Vs travel 0.12 km/s faster than in AFM. These absolute velocity differences correspond to respectively only 1.5% and 1.8% relative difference.

[15] If we assume a linear dependence of the seismic properties along the $(Mg,Fe)SiO_3$ solid solution, then for a pyrolitic mantle with an average 8 at. % ferrous iron in perovskite [*Kesson et al.*, 1998] the difference in seismic wave velocities between the high-spin and low-spin configurations will be of only 0.12% for Vp and 0.15% for Vs. Even considering a larger iron content, like 15 at. %, which is closer to the upper acceptable limit for pyrolite, these differences go up to only 0.23% and 0.29% respectively for Vp and Vs. These values are definitely too low to be detectable using current seismological techniques and body waves, as they would only lead to very small travel time differences in waves bottoming at different depths. Also, since the transition takes place over a large pressure range it will not produce any reflectors detectable with seismic body waves. It was shown based on thermodynamical considerations and later observed in experimental measurements that during the spin transitions an elastic anomaly develops that leads to a considerable reduction in wave velocities [*Speziale et al.*, 2007]. However it is also highly temperature-dependent such that at lower mantle temperatures where the iron spin transition takes place in perovskite the variation of the seismic properties will be smooth and undetectable seismically.

[16] If the bulk seismic wave velocities are not strongly affected by the spin transition in Fe-bearing perovskite, things are different when one looks at the seismic anisotropy (Figure 1). The $MgSiO_3$ and the orthorhombic high-spin $FeSiO_3$ perovskites, show similar anisotropy patterns. The minimum velocities are along the normal to the X direction and the maximum velocities are along the X direction. The amount of Vp anisotropy is on the order of 5–7% for both $MgSiO_3$ and $FeSiO_3$. The Vs anisotropy is different between the two compositions, and more importantly between the high-spin and the low-spin phases of iron-bearing silicate. The HS $FeSiO_3$ structures have Vs anisotropies up to 1.08% (AFM) and 1.28% (FM); the low-spin $FeSiO_3$ and $MgSiO_3$ have Vs anisotropy up to respectively 2.75% and 2.56%. Consequently alloying Mg-perovksite with the HS Fe or with LS Fe has opposite effects: HS tends to decrease the anisotropy relative to pure $MgSiO_3$ while LS enhances this anisotropy.

[17] Moreover, the patterns of anisotropy for both Vp and Vs between the high-spin and the low-spin Fe phases are significantly different. The bulk of the lower mantle is highly isotropic, with deviations of only about 0.5%, though there are regions where a certain seismic anisotropy is observed, like at the top, close to the transition zone [*Wookey et al.*, 2002] and at the bottom, close to the boundary with the D″ layer [*Cornier*, 1999; *Kendall and Silver*, 1998; *Karato and Karki*, 2001; *Kustowski et al.*, 2008] with values going up to about 1%. In these settings lattice preferred orientation could develop because of the convection cells and would align a majority of Fe-bearing perovskite crystals. Differences in spin state would induce differences in the seismic anisotropy pattern between the top and the bottom parts of the lower mantle. Therefore, a pattern like this should be detectable in observations of anisotropy at the base of the transition zone and into the lower mantle [e.g., *Wookey et al.*, 2002] and the D″ region for waves with different turning depths, even for pyrolitic Fe concentrations. Due to the pattern of fast and slow velocities (Figure 2) it could also introduce larger travel time differences for waves with different turning depths than suggested above. That then needs to be taken into account as corrections in tomographic studies. Moreover our results show that lateral heterogeneities that induce these fluctuations of the anisotropy visible in tomographic studies can be due not only to mineralogical and chemical variations but also to iron spin variations (induced by differences in temperature and/or iron distribution and concentration) coupled with lattice preferred orientation.

[18] **Acknowledgments.** The work was facilitated by the PROCOPE exchange program. The calculations were performed on the jade machine at CINES under computational grant stl2816.

References

Badro, J., et al. (2004), Electronic transitions in perovskite: Possible nonconvecting layers in the lower mantle, *Science*, *305*, 383–386.

Baroni, S., S. de Gironcoli, A. Dal Corso, and P. Giannozzi (2001), Phonons and related crystal properties from density-functional perturbation theory, *Rev. Mod. Phys.*, *73*, 515–562.

Baroni, S., P. Giannozzi, and A. Testa (1987), Green's-function approach to linear response in solids, *Phys. Rev. Lett.*, *58*, 1861–1864.

Bengtson, A., K. Persson, and D. Morgan (2008), Ab initio study of the composition dependence of the pressure induced spin crossover in perovskite $(Mg_{1-x}, Fe_x)SiO_3$, *Earth Planet. Sci. Lett.*, *265*, 535–545.

Caracas, R., and R. E. Cohen (2005), Effect of chemistry on the stability and elasticity of the perovskite and post-perovskite phases in the $MgSiO_3$-$FeSiO_3$-Al_2O_3 system and implications for the lowermost mantle, *Geophys. Res. Lett.*, *32*, L16310, doi:10.1029/2005GL023164.

Caracas, R., and R. E. Cohen (2007), Effect of chemistry on the physical properties of perovskite and post-perovskite, in *Post-Perovskite: The Last Mantle Phase Transition*, *Geophys. Monogr. Ser.*, vol. 174, edited by K. Hirose et al., pp. 115–128, AGU, Washington, D. C.

Caracas, R., and R. E. Cohen (2008), Ferrous iron in post-perovskite from first-principles calculations, *Phys. Earth Planet. Inter.*, *168*, 147–152.

Cohen, R. E. (1987), Elasticity and equation of state of $MgSiO_3$ perovskite, *Geophys. Res. Lett.*, *14*, 1053–1056.

Cornier, V. F. (1999), Anisotropy of heterogeneity scale lengths in the lower mantle from PKIKP precursors, *Geophys. J. Int.*, *136*, 373–384.

Fang, C., and R. Ahuja (2008), Local structure and electronic-spin transition of Fe-bearing $MgSiO_3$ perovskite under conditions of the Earth's lower mantle, *Phys. Earth Planet. Inter.*, *166*, 77–82.

Gonze, X., and C. Lee (1997), Dynamical matrices, born effective charges, dielectric permittivity tensors, and interatomic force constants from density-functional perturbation theory, *Phys. Rev. B*, *55*, 10,355–10,368.

Gonze, X., et al. (2002). First-principles computation of material properties: The ABINIT software project, *Comput. Mater. Sci.*, *25*, 478–492.

Gonze, X., G.-M. Rignanese, and R. Caracas (2005a), First-principles studies of the lattice dynamics of crystals, and related properties, *Z. Kristallogr.*, *220*, 458–472.

Gonze, X., et al. (2005b), A brief introduction to the ABINIT software package, *Z. Kristallogr.*, *220*, 558–562.

Hamann, D., X. Wu, K. M. Rabe, and D. Vanderbilt (2005), Metric tensor formulation of strain in density-functional perturbation theory, *Phys. Rev. B*, *71*, 035117, doi:10.1103/PhysRevB.71.035117.

Hohenberg, P., and W. Kohn (1964), Inhomogenous electron gas, *Phys. Rev.*, *136*, B864–B871.

Jackson, J. M., et al. (2005), A synchrotron Mössbauer spectroscopy study of $(Mg,Fe)SiO_3$ perovskite up to 120 GPa, *Am. Mineral.*, *90*, 199–205.

Jackson, J. M., W. Sturhahn, O. Tschauner, M. Lerche, and Y. Fei (2009), Behavior of iron in (Mg,Fe)SiO_3 post-perovskite assemblages at Mbar pressures, *Geophys. Res. Lett.*, *36*, L10301, doi:10.1029/2009GL037815.

Karato, S., and B. B. Karki (2001), Origin of lateral variation of seismic wave velocities and density in the deep mantle, *J. Geophys. Res*, *106*, 21,771–21,783.

Karki, B. B., et al. (1998), Elastic properties of orthorhombic $MgSiO_3$ perovskite at lower mantle pressures, *Am. Mineral.*, *82*, 635–638.

Kendall, J.-M., and P. G. Silver (1998), Investigating causes of D″ anisotropy, in *The Core-Mantle Boundary Region*, *Geodyn. Ser.*, vol. 28, edited by J. X. Mitrovica and B. L. A. Vermeersen, pp. 97–118, AGU, Washington, D. C.

Kesson, S. E., J. D. Fitz Gerald, and J. M. Shelley (1998), Mineralogy and dynamics of a pyrolite mantle, *Nature*, *393*, 252–255.

Kiefer, B., L. Stixrude, and R. M. Wentzcovitch (2002), Elasticity of (Mg,Fe)SiO_3-perovskite at high pressures, *Geophys. Res. Lett.*, *29*(11), 1539, doi:10.1029/2002GL014683.

Kustowski, B., G. Ekström, and A. M. Dziewoński (2008), Anisotropic shear-wave velocity structure of the Earth's mantle: A global model, *J. Geophys. Res.*, *113*, B06306, doi:10.1029/2007JB005169.

Li, J., et al. (2004), Electronic spin state of iron in lower mantle perovskite, *Proc. Natl. Acad. Sci. U. S. A.*, *101*, 14,027–14,030.

Li, J., et al. (2006), Pressure effect on the electronic structure of iron in (Mg,Fe)(Si,Al)O_3 perovskite: A combined synchrotron Mössbauer and X-ray emission spectroscopy study up to 100 GPa, *Phys. Chem. Miner.*, *33*, 575–585.

Lin, J.-F., and T. Tsuchiya (2008), Spin transition of iron in the Earth's lower mantle, *Phys. Earth Planet. Inter.*, *170*, 248–259.

Lin, J.-F., et al. (2005), Spin transition of iron in magnesiowüstite in the Earth's lower mantle, *Nature*, *436*, 377–380.

Lin, J.-F., et al. (2007), Spin transition zone in Earth's lower mantle, *Science*, *317*, 1740–1743.

Lin, J.-F., et al. (2008), Intermediate-spin ferrous iron in lowermost mantle post-perovskite and perovskite, *Nat. Geosci.*, *1*, 688–691.

McCammon, C., et al. (2008), Stable intermediate-spin ferrous iron in lower-mantle perovskite, *Nat. Geosci.*, *1*, 684–687.

Monkhorst, H. J., and J. D. Pack (1976), Special points for Brillouin-zone integrations, *Phys. Rev. B*, *13*, 5188–5192.

Oganov, A. R., J. P. Brodholt, and G. D. Price (2001), The elastic constants of $MgSiO_3$ perovskite at pressures and temperatures of the Earth's mantle, *Nature*, *411*, 934–937.

Payne, M. C., M. P. Teter, D. C. Allan, T. A. Arias, and J. D. Joannopoulos (1992), Iterative minimization techniques for ab initio total-energy calculations: Molecular dynamics and conjugate gradients, *Rev. Mod. Phys.*, *64*, 1045–1097.

Sinelnikov, Y. D., G. Chen, D. R. Neuville, M. T. Vaughan, and R. C. Liebermann (1998), Ultrasonic shear wave velocities of $MgSiO_3$ perovskite at 8 GPa and 800 K and lower mantle composition, *Science*, *281*, 677–679.

Speziale, S., V. E. Lee, S. M. Clark, J. F. Lin, M. P. Pasternak, and R. Jeanloz (2007), Effects of Fe spin transition on the elasticity of (Mg, Fe)O magnesiowüstites and implications for the seismological properties of the Earth's lower mantle, *J. Geophys. Res.*, *112*, B10212, doi:10.1029/2006JB004730.

Stackhouse, S., J. P. Brodholt, and G. D. Price (2006), Elastic anisotropy of $FeSiO_3$ end-members of the perovskite and post-perovskite phases, *Geophys. Res. Lett.*, *33*, L01304, doi:10.1029/2005GL023887.

Stackhouse, S., J. P. Brodholt, and G. D. Price (2007), Electronic spin transitions in iron-bearing $MgSiO_3$ perovskite, *Earth Planet. Sci. Lett.*, *253*, 282–290.

Umemoto, K., R. M. Wentzcovitch, Y. G. Yu, and R. Requist (2008), Spin transition in (Mg,Fe)SiO_3 perovskite under pressure, *Earth Planet. Sci. Lett.*, *276*, 198–206.

Wentzcovitch, R. M., B. B. Karki, M. Cococcioni, and S. de Gironcoli (2004), Thermoelastic properties of $MgSiO_3$ perovskite: Insights on the nature of Earth's lower mantle, *Phys. Rev. Lett.*, *92*, 018501.

Wookey, J., J.-M. Kendall, and G. Barruol (2002), Mid-mantle deformation inferred from seismic anisotropy, *Nature*, *415*, 777–780.

Yeganeh-Haeri, A., D. J. Weidner, and E. Ito (1989), Elasticity of $MgSiO_3$ in the perovskite structure, *Science*, *243*, 787–789.

Zhang, F., and A. R. Oganov (2006), Valence state and spin transitions of iron in Earth's mantle silicates, *Earth Planet. Sci. Lett.*, *249*, 436–443.

R. Caracas, Laboratoire de Sciences de la Terre, UMR 5570, Ecole Normale Supérieure de Lyon, CNRS, 46, allée d'Italie, F-69364 Lyon CEDEX, France. (razvan.caracas@ens-lyon.fr)

D. Mainprice, Géosciences Montpellier, UMR 5243, Université Montpellier 2, CNRS, Pl. Eugène Bataillon, F-34095 Montpellier CEDEX, France.

C. Thomas, Institut für Geophysik, Westfälische Wilhelms Universität Münster, Corrensstrasse 24, D-48149 Münster, Germany.